Few-layer MoS_2-deposited microfiber as highly nonlinear photonic device for pulse shaping in a fiber laser [Invited]

Ai-Ping Luo,[1] Meng Liu,[1] Xu-De Wang,[1] Qiu-Yi Ning,[1] Wen-Cheng Xu,[1,2] and Zhi-Chao Luo[1,*]

[1]*Guangdong Provincial Key Laboratory of Nanophotonic Functional Materials and Devices, School of Information and Optoelectronic Science and Engineering, South China Normal University, Guangzhou, Guangdong 510006, China*
[2]*e-mail: xuwch@scnu.edu.cn*
**Corresponding author: zcluo@scnu.edu.cn*

Received January 6, 2015; revised February 12, 2015; accepted February 15, 2015;
posted February 17, 2015 (Doc. ID 231632); published April 1, 2015

Two-dimensional (2D) materials have emerged as attractive mediums for fabricating versatile optoelectronic devices. Recently, few-layer molybdenum disulfide (MoS_2), as a shining 2D material, has been discovered to possess both the saturable absorption effect and large nonlinear refractive index. Herein, taking advantage of the unique nonlinear optical properties of MoS_2, we fabricated a highly nonlinear saturable absorption photonic device by depositing the few-layer MoS_2 onto the microfiber. With the proposed MoS_2 photonic device, apart from the conventional soliton patterns, the mode-locked pulses could be shaped into some new soliton patterns, namely, *multiple soliton molecules*, *localized chaotic multipulses*, and *double-scale soliton clusters*. Our findings indicate that the few-layer MoS_2-deposited microfiber could operate as a promising highlynonlinear photonic device for the related nonlinear optics applications.

OCIS codes: (160.4330) Nonlinear optical materials; (250.5530) Pulse propagation and temporal solitons; (140.3510) Lasers, fiber; (140.4050) Mode-locked lasers.
http://dx.doi.org/10.1364/PRJ.3.000A69

1. INTRODUCTION

The discovery of two-dimensional (2D) layered materials opens up new opportunities for next-generation photonics technology [1–4]. Interests in investigating optoelectronic and photonic applications of 2D materials are strongly stimulated by their unique electronic and optical properties. Graphene [5,6], as a typical 2D material, has received the most attention for applications in various fields in recent years. Regarding the photonics applications, the unique electronic band structure of graphene makes it possess many excellent optical properties such as ultra-wideband saturable absorption and ultrafast nonlinear optical response [7–16]. These features of graphene are especially suitable for generation of ultrafast pulses in lasers [17,18]. Indeed, by introducing graphene into the laser cavity, so far the high-quality mode-locked [19–27] or *Q*-switched [28–32] pulses could be readily generated in lasers. However, despite the advantages of graphene mentioned above, graphene also shows several intrinsic shortcomings, namely weak absorption coefficiency and zero bandgap that would degenerate its light modulation ability and limit its potential applications in the related photonics fields requiring strong light–matter interaction.

Triggered by the successful story of graphene, the nonlinear optical responses of other 2D materials such as topological insulators (TIs) [33–35] and atomic layered transition-metal dichalcogenides (TMDs) [36,37] were heavily investigated recently. With TI saturable absorbers (SAs), the pulsed lasers operating in passive mode-locking [38–47] and *Q*-switching regimes [48–53] could be obtained at different wavebands. As for representative 2D TMDs, few-layer molybdenum disulfide (MoS_2) presents interesting layer-dependent electronic and optical properties when exfoliated from its bulk type [54,55]. It has been revealed that in MoS_2 there exists a transition from an indirect bandgap in the bulk type to a direct bandgap in the monolayer (or few-layer) state. The characteristics of the layer-dependent bandgap structure, which are distinct from graphene, put the 2D MoS_2 materials into an important position for fabricating flexible optoelectronic devices [56,57]. Recently, few-layer MoS_2 was also found to possess saturable absorption effect, which was similar to graphene [58–61]. However, recent advances in the investigations of MoS_2 show that few-layer MoS_2 possesses stronger saturable absorption response than graphene [58], prompting it to act as a promising material for nanophotonic devices, such as SAs and optical switches. Enlightened by the discovery of its saturable absorption effect, the photonic applications of few-layer MoS_2 are now under intensive investigations for the ultrafast laser community [62–71] because of the strong saturable absorption ability for generating ultrashort pulses. Zhang *et al.* demonstrated the broadband saturable absorption of few-layer MoS_2 at 400, 800, and 1060 nm wavebands and achieved passive mode-locking operation in an Yb-doped fiber laser at 1 μm [59]. Then the femtosecond pulse from an erbium-doped fiber (EDF) laser operating at the 1550 nm waveband with a filmy few-layer MoS_2 SA was first revealed by our group [62], which further expands the saturable absorption waveband of few-layer MoS_2. So far, a wideband saturable absorption from 400 nm to 2.1 μm has been demonstrated with few-layer MoS_2 [59,60,62–65]. It is shown that the broadband saturable absorption could be

induced by the existence of the defects in the few-layer MoS_2 [60]. In addition to the saturable absorption, the large nonlinear refractive index was also demonstrated in few-layer MoS_2 [72]. Therefore, combining the two nonlinear optical properties of saturable absorption and large nonlinear refractive index, it is expected that the few-layer MoS_2 could be potentially used to fabricate highly nonlinear saturable absorption photonic devices for investigations of nonlinear optics phenomena.

On the other hand, the passively mode-locked soliton fiber lasers, which could be regarded as nonlinear dissipative systems, have been demonstrated as excellent platforms for investigating versatile soliton dynamics and nonlinear phenomena. By skillfully selecting the laser cavity parameters, various soliton dynamics could be observed in passively mode-locked fiber lasers, namely vector solitons [73–78], dissipative soliton resonance [79–85], rogue waves [86,87], and dark/bright-dark solitons [88,89]. The investigations of soliton nonlinear phenomena contribute to further understanding of the physical features of optical solitons. Among all the cavity parameters of mode-locked lasers, the intracavity nonlinear effect is vital to the evolution of optical solitons. It has been demonstrated that, in addition to the saturable absorption effect, under the condition of high cavity nonlinearity the mode-locked soliton in fiber lasers would be shaped into versatile multisoliton patterns [90–93]. Generally, the effect of high cavity nonlinearity in the lasers is achieved by increasing the intracavity lasing power, which requires a correspondingly high pumping power level. However, from another point of view, if a proper highly nonlinear photonic device is employed in the fiber laser, the requirement of high pump power for investigating the dynamics of soliton patterns could be definitely relaxed. Therefore, considering the excellently nonlinear optical properties of few-layer MoS_2, it would be curious to see whether some interesting soliton patterns could be generated in a fiber laser with a MoS_2 photonic device.

In this contribution, we fabricated a MoS_2 photonic device by depositing the MoS_2 onto a microfiber. Since the interaction length between the few-layer MoS_2 and propagation light via evanescent field is long enough, the nonlinear effect of the proposed microfiber-based MoS_2 photonic device is much larger than those of fiber core interaction ones. By introducing the fabricated microfiber-based MoS_2 photonic device which simultaneously offers highly nonlinear and saturable absorption effects, the mode-locked soliton in the fiber laser could be shaped into various soliton patterns. We have identified six types of soliton patterns which are characterized by the temporal evolutions, for example, multiple soliton molecules, localized chaotic multipulses, and double-scale soliton clusters. For the given experimental conditions, the transition from one soliton state to another could be controlled by adjusting the pump power or the polarization controllers (PCs). The obtained results suggest that the few-layer MoS_2-deposited microfiber could be indeed a good candidate for highly nonlinear photonic devices for application fields such as ultrafast nonlinear optics.

2. FABRICATION AND CHARACTERISTICS OF MICROFIBER-BASED MoS_2 PHOTONIC DEVICE

The MoS_2 nanosheets were synthesized by employing a cost-effective and convenient hydrothermal intercalation and exfoliation method [55]. To characterize the morphology of the MoS_2 nanosheets, the scanning electron microscopy (SEM) image of the MoS_2 is shown in Fig. 1(a), in which we can identify the crystalline structure. Figure 1(b) illustrates the Raman spectrum of the as-prepared MoS_2. Both the in-plane vibrational mode E^1_{2g} at 382.4 cm^{-1} and the out-of-plane vibrational mode A_{1g} at 406.3 cm^{-1} could be observed, which is well consistent with our previous report [62].

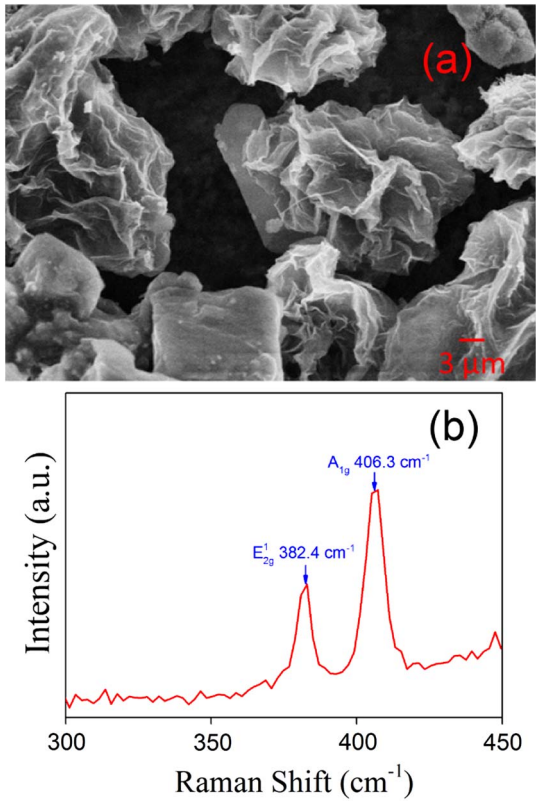

Fig. 1. (a) SEM image of MoS_2; (b) Raman spectrum of exfoliated MoS_2.

Here, the MoS_2 nanosheets were dispersed uniformly in an alcohol solution with a concentration of ~0.02 mg/mL before the process of optical deposition. Then the microfiber was drawn from the standard single-mode fiber (SMF) by using the flame-brushing technique [94]. The diameter of the microfiber is ~9 μm in this experiment. The experimental setup of optical deposition for fabrication of the microfiber-based MoS_2 photonic device and the detailed process have been described in [39]. It should be noted that the deposition process was *in situ* observed by the microscope with a magnification of 100-fold. Therefore, when the amount of MoS_2 nanosheets was properly deposited onto the microfiber, we stopped the deposition process and the fabrication of the microfiber-based MoS_2 photonic device was accomplished. The as-prepared few-layer MoS_2 deposited microfiber is shown in Fig. 2(a). As can be seen here, the MoS_2 nanosheets were deposited well around the microfiber, whose deposition length of MoS_2 is estimated to be ~900 μm. By injecting visible light into the microfiber-based MoS_2 photonic device, the scattering evanescent field around the waist region could be observed, as shown in Fig. 2(b). In order to characterize the saturable absorption effect of the prepared microfiber-based MoS_2 photonic device, the power-dependent transmission technique

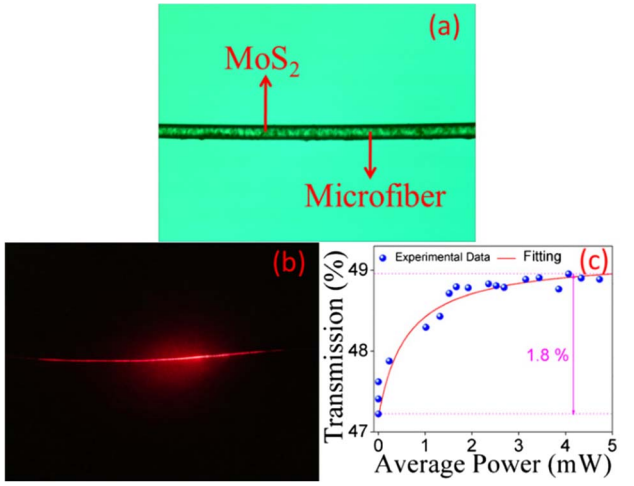

Fig. 2. (a) Microscopy image of the as-prepared few-layer MoS_2 deposited microfiber (black portion: MoS_2); (b) scattering evanescent field around the waist region of microfiber; (c) measured saturable absorption curve and the corresponding fitting curve.

was introduced, whose setup is the same as that we previously used [39]. The results are shown in Fig. 2(c). Here, the nonsaturable loss is ~51.1% and the modulation depth is ~1.8%, which is sufficient for passive mode-locking of a fiber laser. In addition, no evident polarization dependent loss of the MoS_2-deposited microfiber was observed, which was measured to be ~0.15 dB in our experiment.

3. LASER SETUP AND PERFORMANCE

First, the prepared few-layer MoS_2-deposited microfiber was incorporated into an EDF laser. The schematic of the passively mode-locked EDF laser is shown in Fig. 3. A segment of ~7 m EDF was used as the gain medium, which was pumped by a 980 nm laser diode with maximum power of ~400 mW. The other fibers used to construct the fiber laser are all standard SMF. The polarization states of propagation light and the phase relationships of the multiple solitons could be adjusted through a pair of PCs. A polarization-independent isolator (PI-ISO) was used to ensure the unidirectional operation of the fiber laser. The cavity length is 40.7 m, corresponding to a fundamental repetition rate of 5.05 MHz. With a 10% fiber coupler, the laser output is monitored by an optical spectrum analyzer (Yokogawa AQ6317C) and an oscilloscope (Tektronix DSA 70804) with a high-speed photodetector (New Focus P818-BB-35F, 12.5 GHz). Moreover, the pulse profiles were measured by a commercial autocorrelator (FR-103XL).

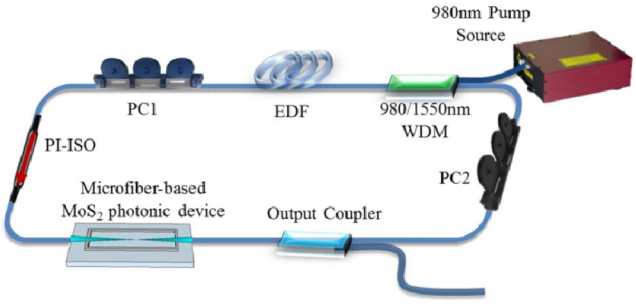

Fig. 3. Schematic of the proposed passively mode-locked EDF laser with a microfiber-based MoS_2 photonic device.

A. Single Soliton

In the experiment, the continuous wave (cw) lasing threshold of the fiber laser is ~10 mW. The mode-locking operating could be easily achieved by simply increasing the pump power due to the saturable absorption ability of few-layer MoS_2. However, as mentioned above, the few-layer MoS_2 possesses a large nonlinear refractive index. Therefore, the fiber laser was always inclined to emit multiple pulses because of the quantization of soliton energy [95]. Nevertheless, by virtue of the pump hysteresis phenomenon [96], the fiber laser still could operate in the single-soliton regime by carefully decreasing the pumping power level. Figure 4 presents the mode-locked spectrum of the single soliton regime at the pump power of 18 mW. Being different from the conventional mode-locked spectrum operating in the anomalous dispersion regime, two strong cw peaks were shown on the mode-locked spectrum. We attributed it to the imperfect mode-locking state under a relatively low pump power. The corresponding pulse-train is shown in Fig. 5. The pulse repetition rate is calculated to be 5.05 MHz, which is in good agreement with the cavity length of 40.7 m. To identify whether there are any fine structures in the pulse profile, we measured the autocorrelation trace of the mode-locked pulse. The measured result is plotted

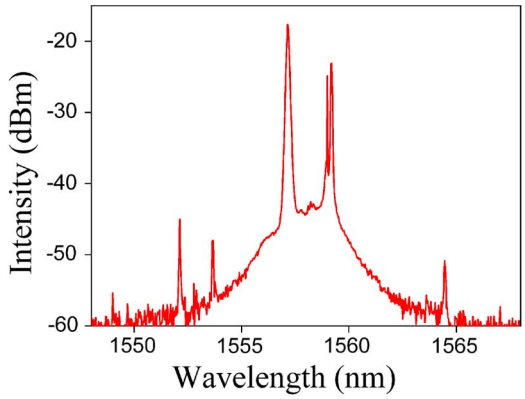

Fig. 4. Mode-locked spectrum of the single soliton regime.

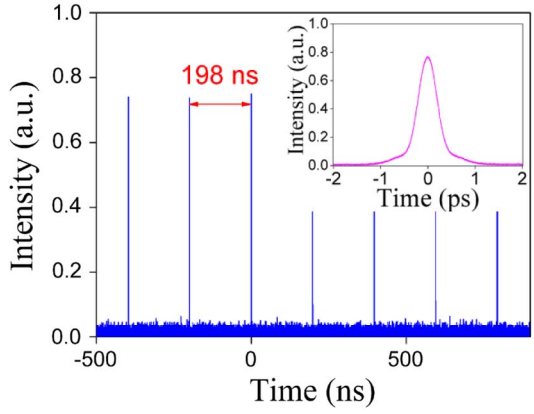

Fig. 5. Pulse-train of single soliton regime. Inset: Autocorrelation trace of single soliton regime.

in the inset of Fig. 5, in which we can see that only a single soliton could be observed.

B. Multiple Soliton Molecules

After achievement of single soliton operation, the pump power was slightly increased to 30 mW. In this case, the multi-soliton oscillation could be easily observed. Figure 6 presents the typical mode-locked spectrum of multisoliton operation. It should be noted that the mode-locked spectrum is similar to that of single soliton operation because of the only slight increase of pump power. The mode-locked pulse train is shown in Fig. 7. Although the pulse repetition rate shown in Fig. 7 seems to be a fundamental one, the fiber laser actually contains five solitons which can be clearly seen by reducing the scanning range to several nanoseconds, as shown in the inset of Fig. 7. Then we measured the pulse profile of the obtained fivesoltions. Surprisingly, it can be seen that three peaks with 950 fs separation were symmetrically shown on the autocorrelation trace, which is the typical characteristic of the soliton molecules, as shown in Fig. 8. The results indicate that the each of the five solitons also consists of two "soliton atoms" inside the molecule; that is, *multiple soliton molecules* are achieved. However, no spectral modulations could be observed on the spectrum of multiple soliton molecules, which could be caused by the independently evolution or flipping phases of the soliton molecules [97]. Note that generally

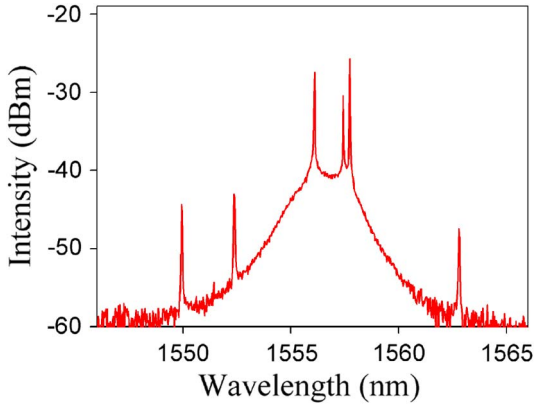

Fig. 6. Typical mode-locked spectrum of multiple soliton molecules.

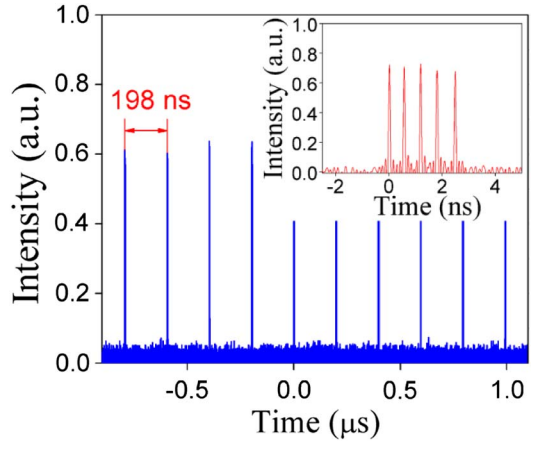

Fig. 7. Pulse-train of multiple soliton molecules. Inset: pulse train under small range.

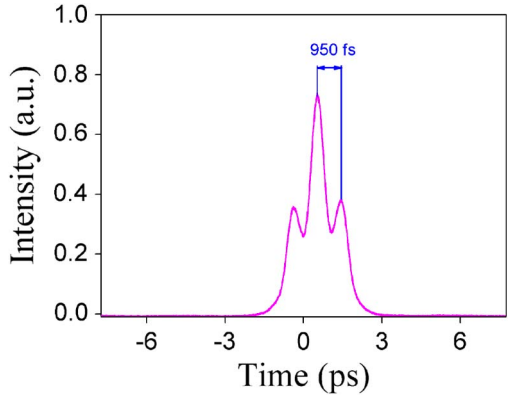

Fig. 8. Autocorrelation trace of multiple soliton molecules.

the generation of soliton molecules in passively mode-locked fiber lasers was observed only with the fundamental repetition rate [98]. That is to say, without a confirmation of the autocorrelation trace, the pulse train shown on the oscilloscope is similar to those of single soliton operation when the conventional soliton molecules are achieved. However, in this experiment, five soliton molecules could be observed under a low pump power level. It should be noted that other numbers of multiple soliton molecules with different pulse separations could be also observed by carefully tuning the pump power level, for example, three soliton molecules. This phenomenon could be attributed to the excellent saturable absorption ability and highly nonlinear effect of few-layer MoS_2 deposited microfiber for strong soliton shaping in the fiber laser.

C. Soliton Flow

When the PCs were carefully rotated and the pump power was tuned to 60.5 mW, the multiple soliton molecules evolved dramatically. In this case, the multiple solitons which were shown in the inset of Fig. 7 could break the localized region and move relatively. Meanwhile, the number of solitons also increased. Under the proper adjustments of PCs, the multiple solitons could move in a regular trend. The oscilloscope traces shows that the multiple solitons evolved into a stable soliton condensed phase and many drifting small solitons, that is, soliton flow [90,99]. It should be noted that the pump power for the formation of soliton flow in our fiber laser under the highly nonlinear circumstance was greatly reduced compared with previous reports, namely, 450 mW [90]. Figure 9 presents a snapshot of the oscilloscope trace of the observed soliton

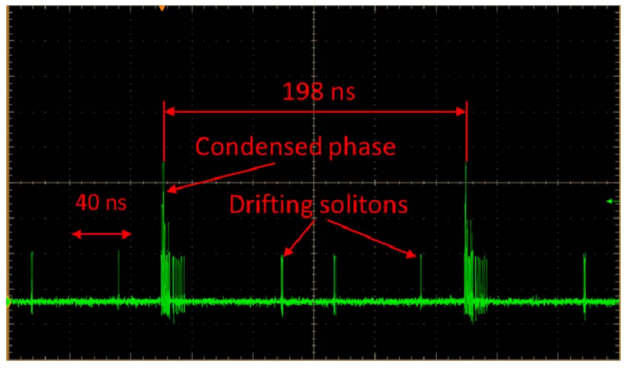

Fig. 9. Pulse train of soliton flow (Media 1).

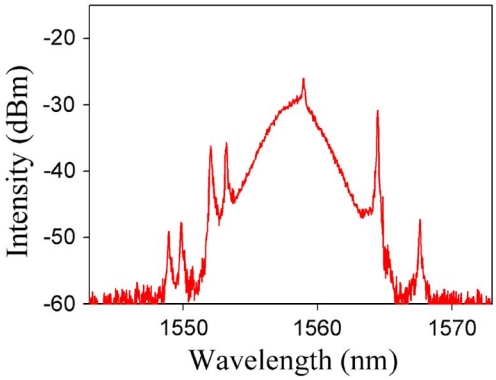

Fig. 10. Spectrum of soliton flow.

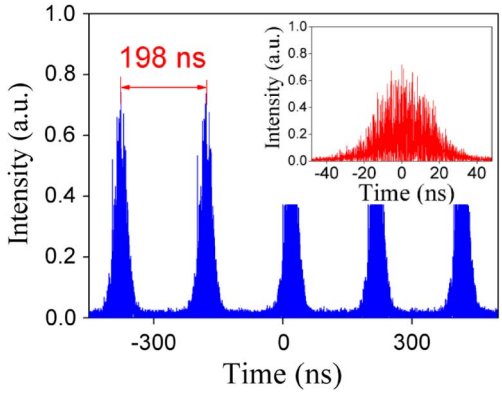

Fig. 11. Pulse train of localized chaotic bunched pulses. Inset: Pulse train under small range.

flow. As summarized in Fig. 9, the soliton flow are composed of three field components: a soliton condensed phase, a lot of isolated drifting solitons, and a noisy cw background [90,99]. When the soliton flow was achieved, on the oscilloscope we could observe that some new solitons arise from the soliton condensed phase and get away from it. Then the generated new solitons drift at different speeds to the next soliton condensed phase, until they finally reach the condensed phase, which is well consistent with the phenomenon of soliton flow. For better clarity, we have also shown the dynamics of soliton flow in Media 1. Figure 10 shows the corresponding spectrum of soliton flow, where the soliton Kelly sidebands could be clearly observed. Note that a cw component always appeared on the mode-locked spectrum of soliton flow. It has been demonstrated that the cw component plays an important role in the interactions among multiple solitons, which is favorable for the generation of soliton flow in fiber lasers [99]. In the experiment, as long as the PCs and the pump power are appropriately, the soliton flow could be frequently observed in our fiber laser.

D. Localized Chaotic Bunched Pulses

Then we kept increasing the pump power to ~155 mW. Correspondingly, the number of mode-locked pulses was further increased. However, the drifting solitons of the soliton slow stopped moving on the oscilloscope. Then by properly rotating the PCs, the multipulse operation would evolve into another interesting soliton pattern, where we can see on the oscilloscope the multiple pulses bunched together. The pulse train and the detailed pulse profile are exhibited in Fig. 11. As characterized in Fig. 11, the envelope of the bunched pulses is similar to that of a Q-switched mode-locking pulse. However, the repetition rate of the pulse envelope is well consistent with the fundamental one. In this case, the bunched pulses are unstable and even chaotic. However, it is worthy of note that the multiple pulses could be localized in tens of nanoseconds under this operation regime, as presented in the inset of Fig. 11. Therefore, we termed this phenomenon as *localized chaotic bunched pulses*. The localized performance of the chaotic bunched pulses could be induced by the strong soliton interactions that avoid the neighboring solitons locating too far to each other. Figure 12 shows the corresponding spectrum of localized chaotic pulses. The central wavelength and the 3 dB spectral bandwidth are 1558.7 and 0.6 nm, respectively. As can be seen here, the cw spectral peaks disappear under the stronger pump power. Nevertheless, there are numerous small spectral spikes on the mode-locked spectrum, which could be caused by the chaotic state of the bunched pulses.

E. Double-Scale Soliton Clusters

By adjusting the pump power to 186 mW, the number of solitons was further increased and the localized chaotic bunched pulses tended to break up. Correspondingly, the cw peak was shown on the spectrum of the mode-locked soliton again and became unstable at this time. Then the multiple solitons generated in the fiber laser moved relatively and finally came together. As the PCs were slightly adjusted, the multiple solitons would bunch together tightly and form a soliton cluster. Figure 13(a) depicts the output pulse-train operating in the cluster regime from our fiber laser. Being distinct from the regular soliton cluster [100], two soliton clusters with different scales could be observed, which we called *double-scale soliton clusters*. The unit of double-scale soliton clusters operated at the fundamental repetition rate. The detailed profile of double-scale soliton clusters is also summarized in Fig. 13(b). It can be seen that the soliton cluster with higher intensity possesses a nearly uniform intensity distribution, while the other one shows a sine-like intensity modulation. The two soliton clusters cover time spans of ~123 and ~75 ns, respectively.

The corresponding mode-locked spectrum of double-scale soliton clusters is shown in Fig. 14. Here, the mode-locked spectrum is smooth and no small spectral spikes could be observed. In addition, apart from the soliton Kelly sidebands, the additional sets of spectral sidebands, which have been known

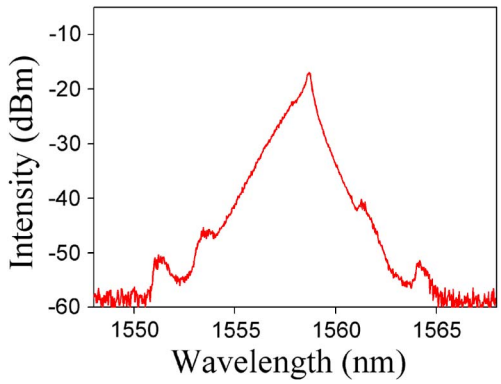

Fig. 12. Spectrum of localized chaotic bunched pulses.

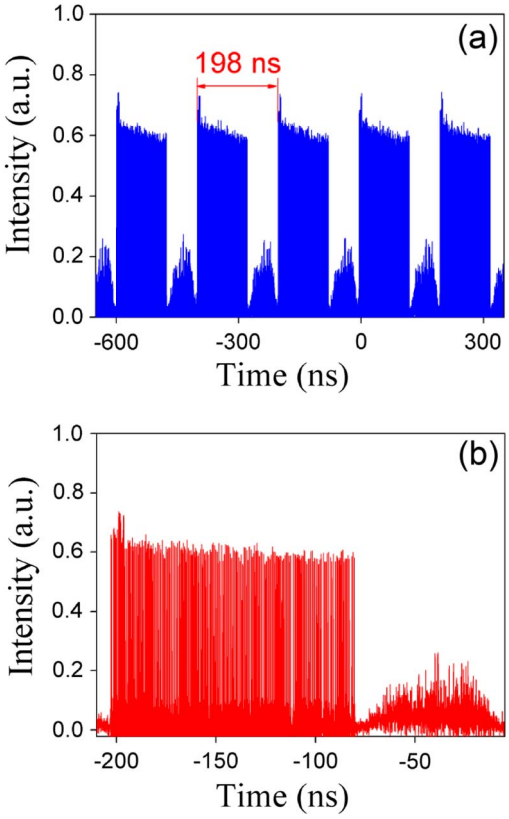

Fig. 13. Pulse trains of double-scale soliton clusters (a) under large range, (b) under small range.

as subsidebands, also appeared on the mode-locked spectrum. The generation of subsidebands could be caused by modulation instability due to the periodic power variation of solitons [101,102]. It should be noted that the energy between the two soliton clusters could be transferred by carefully adjusting the PCs. That is, the double-scale soliton clusters could evolve into a single-scale soliton cluster (regular one) or harmonic clusters, as characterized in Figs. 15(a) and 15(b), respectively.

F. Multiple Solitons Occupying the Whole Cavity

Generally, the number of the solitons circulating in the laser cavity is directly proportional to the pumping lower level due to the soliton energy quantization. In order to obtain plentiful

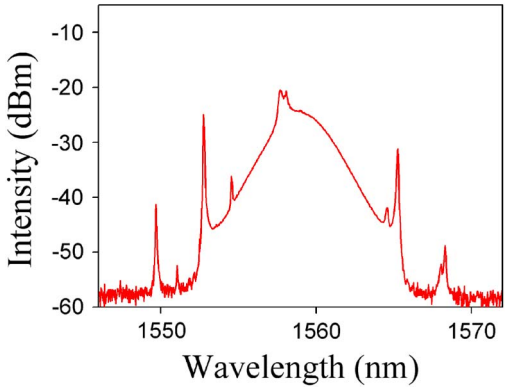

Fig. 14. Mode-locked spectrum of double-scale soliton clusters.

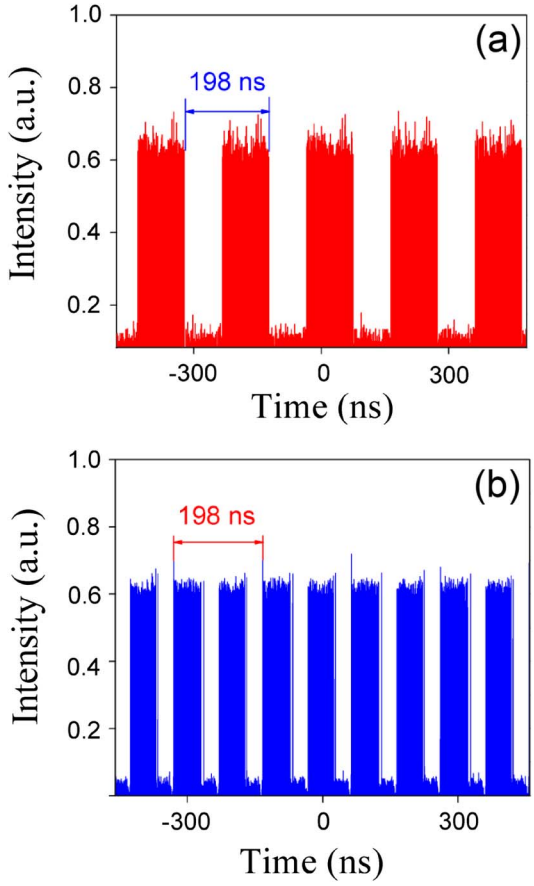

Fig. 15. (a) Single-scale soliton cluster at fundamental repetition rate; (b) harmonic soliton clusters.

solitons, the pump power was then adjusted to be 200 mW. During the process of increasing pump power, the soliton clusters first broke up and distributed along the laser cavity. Then the existent solitons further split, and thus the new solitons were generated. Finally, all the solitons could irregularly occupy all the available space along the laser cavity. Figure 16 shows the recorded oscilloscope trace in the case of the multiple solitons occupying the whole cavity. Here, it can be clearly seen that both the pulse separations and intensities are not uniform, which is different from the harmonic mode-locking

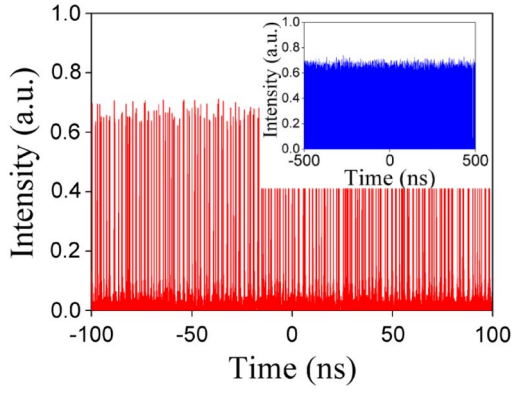

Fig. 16. Recorded oscilloscope trace in the case of the multiple solitons occupying the whole cavity. Inset: Pulse train under 1000 ns range.

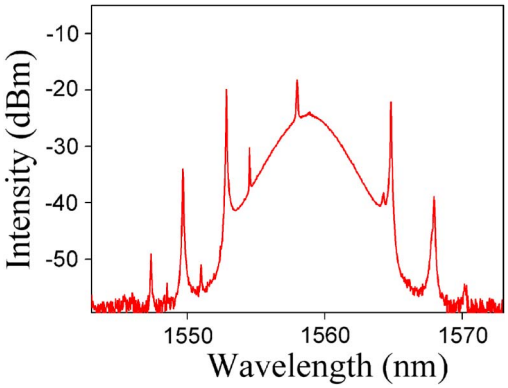

Fig. 17. Spectrum of multiple solitons occupying the whole cavity.

state [39,65,103]. For better clarity, the pulse train measured under the 1000 ns range is also presented in the inset of Fig. 16. In addition, the pulse number was estimated to be 193 in the laser cavity. Note that the pump power for the generation of multiple solitons occupying the whole cavity is ~200 mW, which is also much lower than that of previous reports [100]. It could be still attributed to the highly nonlinear properties of few-layer MoS_2 deposited microfiber, which is beneficial for soliton splitting in fiber lasers. It should be noted that, when the pump power was set to be higher than 200 mW, the soliton patterns also operated among the 6 patterns except for the different output powers. The corresponding mode-locked spectrum with a 3 dB spectral bandwidth of 3.27 nm is shown in Fig. 17. It can be seen that a cw component still appeared on the spectrum, which would facilitate the multisoliton operation in a stable regime [104].

4. DISCUSSION

In the experiment, it was found that various soliton patterns could be easily obtained by simply adjusting the pump power or/and PCs. As we know, the few-layer MoS_2 simultaneously offers both the saturable absorption ability and large nonlinear refractive index. Here, by using the microfiber-based scheme functioning with the evanescent field, the nonlinear effect could be greatly enhanced by extending the interaction length between the propagation light and few-layer MoS_2 in comparison with the filmy type SAs. Under the condition of highly nonlinear effect, the mode-locked soliton would split some excessive energy to balance the accumulated cavity nonlinearity even if the pump power level is low. The split optical waves, despite their small energies, could be reshaped into new solitons due to the saturable absorption ability of few-layer MoS_2. It is worthy of note that in fiber lasers mode locked by the artificial saturable absorption effect, that is, nonlinear polarization rotation and nonlinear optical loop mirror techniques, the optical waves could be shaped into mode-locked soliton pulses only at some specific polarization states of propagation light. However, in this experiment the soliton splitting and saturable absorption occur simultaneously in a single photonic device (few-layer MoS_2-deposited microfiber) independent of polarization states, which is very beneficial for the formation of multiple solitons. Then, all the generated solitons form versatile patterns via interactions among the solitons, continuous waves, and dispersive waves. Therefore, the above-mentioned factors could be responsible for easy observation of various soliton patterns by introducing a highly nonlinear MoS_2-deposited photonic device into a fiber laser.

On the other hand, the experimental results have suggested that the few-layer MoS_2-deposited microfiber could be a good candidate of highly nonlinear photonic device for investigations of various soliton nonlinear phenomena. Therefore, it is expected that other nonlinear soliton dynamics, such as rogue waves [86,87], and dissipative soliton resonance [79–85] could be also observed conveniently by employing such a highly nonlinear MoS_2 photonic device into the laser cavity. In addition, other 2D materials, such as graphene and TI, have also been demonstrated to possess large nonlinear refractive index [105,106]. Thus, the proposed photonic device could be replaced by depositing other 2D materials onto the microfiber for studying the soliton dynamics in fiber lasers. Finally, it should be noted that no evident polarization-dependent loss could be observed with the microfiber-based MoS_2 photonic device if they are deposited uniformly onto the microfiber. As a result, we also could investigate the vector nature of the versatile soliton patterns generated with the MoS_2-deposited microfiber [92], which would further reveal the fundamental physics of soliton patterns.

5. CONCLUSION

In summary, we have investigated the formation of various soliton patterns with a highly nonlinear saturable absorption photonic device by depositing the few-layer MoS_2 onto the microfiber. Taking advantage of both the highly nonlinear effect and saturable absorption generated by the microfiber-based MoS_2 photonic device, different soliton patterns such as multiple soliton molecules, localized chaotic multipulses, and double-scale soliton clusters could be easily observed although the pump power was not high. The observed results would further enhance the understanding of fundamental physics and dynamics of versatile soliton patterns and demonstrate that the MoS_2-deposited microfiber is indeed an excellent highlynonlinear photonic device for a myriad of nonlinear optoelectronic applications.

ACKNOWLEDGMENTS

This work was supported in part by the National Natural Science Foundation of China (Grant Nos. 11474108, 61378036, 61307058, 11304101, 11074078), the PhD Start-up Fund of Natural Science Foundation of Guangdong Province, China (Grant No. S2013040016320), and the Scientific and Technological Innovation Project of Higher Education Institute, Guangdong, China (Grant No. 2013KJCX0051). Z.-C. Luo acknowledges the financial support from the Guangdong Natural Science Funds for Distinguished Young Scholar, and the Zhujiang New-star Plan of Science & Technology in Guangzhou City (Grant No. 2014J2200008).

REFERENCES

1. K. S. Novoselov, D. Jiang, F. Schedin, T. J. Booth, V. V. Khotkevich, S. V. Morozov, and A. K. Geim, "Two-dimensional atomic crystals," Proc. Nat. Acad. Sci. **102**, 10451–10453 (2005).
2. F. Bonaccorso, Z. Sun, T. Hasan, and A. C. Ferrari, "Graphene photonics and optoelectronics," Nat. Photonics **4**, 611–622 (2010).
3. G. Eda and S. A. Maier, "Two-dimensional crystals: managing light for optoelectronics," ACS Nano **7**, 5660–5665 (2013).

4. S. Z. Butler, S. M. Hollen, L. Cao, Y. Cui, J. A. Gupta, H. R. Gutiérrez, T. F. Heinz, S. S. Hong, J. Huang, A. F. Ismach, E. Johnston-Halperin, M. Kuno, V. V. Plashnitsa, R. D. Robinson, R. S. Ruoff, S. Salahuddin, J. Shan, L. Shi, M. G. Spencer, M. Terrones, W. Windl, and J. E. Goldberger, "Progress, challenges, and opportunities in two-dimensional materials beyond graphene," ACS Nano **7**, 2898–2926 (2013).
5. A. K. Geim and K. S. Novoselov, "The rise of graphene," Nat. Mater. **6**, 183–191 (2007).
6. Q. Bao and K. P. Loh, "Graphene photonics, plasmonics, and broadband optoelectronic devices," ACS Nano **6**, 3677–3694 (2012).
7. Q. L. Bao, H. Zhang, Y. Wang, Z. Ni, Y. Yan, Z. Shen, K. P. Loh, and D. Y. Tang, "Atomic layer graphene as saturable absorber for ultrafast pulsed laser," Adv. Funct. Mater. **19**, 3077–3083 (2009).
8. H. Zhang, Q. Bao, D. Tang, L. Zhao, and K. Loh, "Large energy soliton erbium-doped fiber laser with a graphene-polymer composite mode locker," Appl. Phys. Lett. **95**, 141103 (2009).
9. Z. Sun, T. Hasan, F. Torrisi, D. Popa, G. Privitera, F. Wang, F. Bonaccorso, D. M. Basko, and A. C. Ferrari, "Graphene mode-locked ultrafast laser," ACS Nano **4**, 803–810 (2010).
10. H. Zhang, D. Y. Tang, R. J. Knize, L. Zhao, Q. Bao, and K. P. Loh, "Graphene mode locked, wavelength tunable, dissipative soliton fiber laser," Appl. Phys. Lett. **96**, 111112 (2010).
11. Z. Q. Luo, M. Zhou, J. Weng, G. M. Huang, H. Y. Xu, C. C. Ye, and Z. P. Cai, "Graphene-based passively *Q*-switched dual-wavelength erbium-doped fiber laser," Opt. Lett. **35**, 3709–3711 (2010).
12. A. Martinez, K. Fuse, and S. Yamashita, "Mechanical exfoliation of graphene for the passive mode-locking of fiber lasers," Appl. Phys. Lett. **99**, 121107 (2011).
13. Z. C. Luo, W. J. Cao, A. P. Luo, and W. C. Xu, "Optical deposition of graphene saturable absorber integrated in a fiber laser using a slot collimator for passive mode-locking," Appl. Phys. Express **5**, 055103 (2012).
14. Z. Zheng, C. Zhao, S. Lu, Y. Chen, Y. Li, H. Zhang, and S. Wen, "Microwave and optical saturable absorption in graphene," Opt. Express **20**, 23201–23214 (2012).
15. Z. Sun, T. Hasan, and A. C. Ferrari, "Ultrafast lasers mode-locked by nanotubes and graphene," Physica E **44**, 1082–1091 (2012).
16. G. Z. Wang, S. F. Zhang, F. A. Umran, X. Cheng, N. N. Dong, D. Coghlan, Y. Cheng, L. Zhang, W. J. Blau, and J. Wang, "Tunable effective nonlinear refractive index of graphene dispersions during the distortion of spatial self-phase modulation," Appl. Phys. Lett. **104**, 141909 (2014).
17. H. Zhang, D. Y. Tang, L. M. Zhao, Q. L. Bao, and K. P. Loh, "Large energy mode locking of an erbium-doped fiber laser with atomic layer graphene," Opt. Express **17**, 17630–17635 (2009).
18. Z. Sun, D. Popa, T. Hasan, F. Torrisi, F. Wang, E. Kelleher, J. Travers, V. Nicolosi, and A. Ferrari, "A stable, wideband tunable, near transform-limited, graphene-mode-locked, ultrafast laser," Nano Res. **3**, 653–660 (2010).
19. Z. B. Liu, X. Y. He, and D. N. Wang, "Passively mode-locked fiber laser based on a hollow-core photonic crystal fiber filled with few-layered graphene oxide solution," Opt. Lett. **36**, 3024–3026 (2011).
20. L. Gui, W. Zhang, X. Li, X. Xiao, H. Zhu, K. Wang, D. Wu, and C. Yang, "Self-assembled graphene membrane as an ultrafast mode-locker in an erbium fiber laser," IEEE Photon. Technol. Lett. **23**, 1790–1792 (2011).
21. Z. Luo, Y. Huang, J. Wang, H. Cheng, Z. Cai, and C. Ye, "Multi-wavelength dissipative-soliton generation in Yb-fiber laser using graphene-deposited fiber-taper," IEEE Photon. Technol. Lett. **24**, 1539–1542 (2012).
22. G. Sobon, J. Sotor, J. Jagiello, R. Kozinski, M. Zdrojek, M. Holdynski, P. Paletko, J. Boguslawski, L. Lipinska, and K. M. Abramski, "Graphene oxide vs. reduced graphene oxide as saturable absorbers for Er-doped passively mode-locked fiber laser," Opt. Express **20**, 19463–19473 (2012).
23. J. Sotor, G. Sobon, and K. M. Abramski, "Scalar soliton generation in all-polarization-maintaining, graphene mode-locked fiber laser," Opt. Lett. **37**, 2166–2168 (2012).
24. A. Martinez and Z. Sun, "Nanotube and graphene saturable absorbers for fibre lasers," Nat. Photonics **7**, 842–845 (2013).
25. S. Huang, Y. Wang, P. Yan, J. Zhao, H. Li, and R. Lin, "Tunable and switchable multi-wavelength dissipative soliton generation in a graphene oxide mode-locked Yb-doped fiber laser," Opt. Express **22**, 11417–11426 (2014).
26. X. Li, Q. Wang, Y. Tang, Z. Yan, Y. Wang, B. Meng, G. Liang, H. Sun, X. Yu, Y. Zhang, and X. Cheng, "Broadband saturable absorption of graphene oxide thin film and its application in pulsed fiber lasers," IEEE J. Sel. Top. Quantum Electron. **20**, 1101107 (2014).
27. A. P. Luo, P. F. Zhu, H. Liu, X. W. Zheng, N. Zhao, M. Liu, H. Cui, Z. C. Luo, and W. C. Xu, "Microfiber-based, highly nonlinear graphene saturable absorber for formation of versatile structural soliton molecules in a fiber laser," Opt. Express **22**, 27019–27025 (2014).
28. D. Popa, Z. Sun, T. Hasan, F. Torrisi, F. Wang, and A. C. Ferrari, "Graphene *Q*-switched, tunable fiber laser," Appl. Phys. Lett. **98**, 073106 (2011).
29. J. Liu, S. Wu, Q. H. Yang, and P. Wang, "Stable nanosecond pulse generation from a graphene-based passively *Q*-switched Yb-doped fiber laser," Opt. Lett. **36**, 4008–4010 (2011).
30. W. J. Cao, H. Y. Wang, A. P. Luo, Z. C. Luo, and W. C. Xu, "Graphene-based, 50 nm wide-band tunable passively *Q*-switched fiber laser," Laser Phys. Lett. **9**, 54–58 (2012).
31. G. Q. Xie, J. Ma, P. Lv, W. L. Gao, P. Yuan, L. J. Qian, H. H. Yu, H. J. Zhang, J. Y. Wang, and D. Y. Tang, "Graphene saturable absorber for *Q*-switching and mode locking at 2 μm wavelength [Invited]," Opt. Mater. Express **2**, 878–883 (2012).
32. H. Ahmad, F. D. Muhammad, M. Z. Zulkifli, and S. W. Harun, "Graphene oxide based saturable absorber for all-fiber *Q*-switching with a simple optical deposition technique," IEEE Photon. J. **4**, 2205–2213 (2012).
33. H. Zhang, C. X. Liu, X. L. Qi, X. Dai, Z. Fang, and S. C. Zhang, "Topological insulators in Bi_2Se_3, Bi_2Te_3 and Sb_2Te_3 with a single Dirac cone on the surface," Nat. Phys. **5**, 438–442 (2009).
34. M. Z. Hasan and C. L. Kane, "Colloquium: topological insulators," Rev. Mod. Phys. **82**, 3045–3067 (2010).
35. X. L. Qi and S. C. Zhang, "Topological insulators and superconductors," Rev. Mod. Phys. **83**, 1057–1110 (2011).
36. J. N. Coleman, M. Lotya, A. O'Neill, S. D. Bergin, P. J. King, U. Khan, K. Young, A. Gaucher, S. De, R. J. Smith, I. V. Shvets, S. K. Arora, G. Stanton, H. Y. Kim, K. Lee, G. T. Kim, G. S. Duesberg, T. Hallam, J. J. Boland, J. J. Wang, J. F. Donegan, J. C. Grunlan, G. Moriarty, A. Shmeliov, R. J. Nicholls, J. M. Perkins, E. M. Grieveson, K. Theuwissen, D. W. McComb, P. D. Nellist, and V. Nicolosi, "Two-dimensional nanosheets produced by liquid exfoliation of layered materials," Science **331**, 568–571 (2011).
37. Q. H. Wang, K. Kalantar-Zadeh, A. Kis, J. N. Coleman, and M. S. Strano, "Electronics and optoelectronics of two-dimensional transition metal dichalcogenides," Nat. Nanotechnol. **7**, 699–712 (2012).
38. C. J. Zhao, H. Zhang, X. Qi, Y. Chen, Z. T. Wang, S. C. Wen, and D. Y. Tang, "Ultra-short pulse generation by a topological insulator based saturable absorber," Appl. Phys. Lett. **101**, 211106 (2012).
39. Z. C. Luo, M. Liu, H. Liu, X. W. Zheng, A. P. Luo, C. J. Zhao, H. Zhang, S. C. Wen, and W. C. Xu, "2 GHz passively harmonic mode-locked fiber laser by a microfiber-based topological insulator saturable absorber," Opt. Lett. **38**, 5212–5215 (2013).
40. C. J. Zhao, Y. H. Zou, Y. Chen, Z. T. Wang, S. B. Lu, H. Zhang, S. C. Wen, and D. Y. Tang, "Wavelength tunable picosecond soliton fiber laser with topological insulator: Bi_2Se_3 as a mode locker," Opt. Express **20**, 27888–27895 (2012).
41. H. Liu, X. W. Zheng, M. Liu, N. Zhao, A. P. Luo, Z. C. Luo, W. C. Xu, H. Zhang, C. J. Zhao, and S. C. Wen, "Femtosecond pulse generation from a topological insulator mode-locked fiber laser," Opt. Express **22**, 6868–6873 (2014).
42. J. Sotor, G. Sobon, W. Macherzynski, P. Paletko, K. Grodecki, and K. M. Abramski, "Mode-locking in Er-doped fiber laser based on mechanically exfoliated Sb_2Te_3 saturable absorber," Opt. Mater. Express **4**, 1–6 (2014).
43. J. Sotor, G. Sobon, K. Grodecki, and K. M. Abramski, "Sub-130 fs mode-locked Er-doped fiber laser based on topological insulator," Opt. Express **22**, 13244–13249 (2014).

44. Y. H. Lin, C. Y. Yang, S. F. Lin, W. H. Tseng, Q. Bao, C. I. Wu, and G. R. Lin, "Soliton compression of the erbium-doped fiber laser weakly started mode-locking by nanoscale *p*-type Bi_2Te_3 topological insulator particles," Laser Phys. Lett. **11**, 055107 (2014).
45. P. Yan, R. Lin, H. Chen, H. Zhang, A. Liu, H. Yang, and S. Ruan, "Topological insulator solution filled in photonic crystal fiber for passive mode-locked fiber laser," IEEE Photon. Technol. Lett. **27**, 264–267 (2015).
46. M. Jung, J. Lee, J. Koo, J. Park, Y. W. Song, K. Lee, S. Lee, and J. H. Lee, "A femtosecond pulse fiber laser at 1935 nm using a bulk-structured Bi_2Te_3 topological insulator," Opt. Express **22**, 7865–7874 (2014).
47. P. G. Yan, R. Y. Lin, S. C. Ruan, A. J. Liu, and H. Chen, "A 2.95 GHz, femtosecond passive harmonic mode-locked fiber laser based on evanescent field interaction with topological insulator film," Opt. Express **23**, 154–164 (2015).
48. Z. Q. Luo, Y. Z. Huang, J. Weng, H. H. Cheng, Z. Q. Lin, B. Xu, Z. Cai, and H. Xu, "1.06 μm *Q*-switched ytterbium-doped fiber laser using few-layer topological insulator $Bi_2 Se_2$ as a saturable absorber," Opt. Express **21**, 29516–29522 (2013).
49. H. Yu, H. Zhang, Y. Wang, C. Zhao, B. Wang, S. Wen, H. Zhang, and J. Wang, "Topological insulator as an optical modulator for pulsed solid-state lasers," Laser Photon. Rev. **7**, L77–L83 (2013).
50. Y. Chen, C. J. Zhao, H. H. Huang, S. Q. Chen, P. H. Tang, Z. T. Wang, S. B. Lu, H. Zhang, S. C. Wen, and D. Y. Tang, "Self-assembled topological insulator: Bi_2Se_3 membrane as a passive *Q*-switcher in an erbium-doped fiber laser," J. Lightwave Technol. **31**, 2857–2863 (2013).
51. Z. Q. Luo, C. Liu, Y. Z. Huang, D. D. Wu, J. Y. Wu, H. Y. Xu, Z. P. Cai, Z. Q. Lin, L. P. Sun, and J. Weng, "Topological-insulator passively *Q*-switched double-clad fiber laser at 2 μm wavelength," IEEE J. Sel. Top. Quantum Electron. **20**, 0902708 (2014).
52. Z. Yu, Y. Song, J. Tian, Z. Dou, H. Guoyu, K. Li, H. Li, and X. Zhang, "High-repetition-rate *Q*-switched fiber laser with high quality topological insulator $Bi_2 Se_2$ film," Opt. Express **22**, 11508–11515 (2014).
53. L. Gao, W. Huang, J. D. Zhang, T. Zhu, H. Zhang, C. J. Zhao, W. Zhang, and H. Zhang, "*Q*-switched mode-locked erbium-doped fiber laser based on topological insulator Bi_2Se_3 deposited fiber taper," Appl. Opt. **53**, 5117–5122 (2014).
54. K. F. Mak, C. Lee, J. Hone, J. Shan, and T. F. Heinz, "Atomically thin MoS_2 : a new direct-gap semiconductor," Phys. Rev. Lett. **105**, 136805 (2010).
55. J. Zheng, H. Zhang, S. Dong, Y. Liu, C. T. Nai, H. S. Shin, H. Y. Jeong, B. Liu, and K. P. Loh, "High yield exfoliation of two-dimensional chalcogenides using sodium naphthalenide," Nat. Commun. **5**, 2995 (2014).
56. B. Radisavljevic, A. Radenovic, J. Brivio, V. Giacometti, and A. Kis, "Single-layer MoS_2 transistors," Nat. Nanotechnol. **6**, 147–150 (2011).
57. B. Radisavljevic, M. B. Whitwicj, and A. Kis, "Integrated circuits and logic operations based on single-layer MoS_2," ACS Nano **5**, 9934–9938 (2011).
58. K. P. Wang, J. Wang, J. T. Fan, M. Lotya, A. O'Neill, D. Fox, Y. Y. Feng, X. Y. Zhang, B. X. Jiang, Q. Z. Zhao, H. Zhang, J. N. Coleman, L. Zhang, and W. J. Blau, "Ultrafast saturable absorption of two-dimensional MoS_2 nanosheets," ACS Nano **7**, 9260–9267 (2013).
59. H. Zhang, S. B. Lu, J. Zheng, J. Du, S. C. Wen, D. Y. Tang, and K. P. Loh, "Molybdenum disulfide (MoS_2) as a broadband saturable absorber for ultra-fast photonics," Opt. Express **22**, 7249–7260 (2014).
60. S. Wang, H. Yu, H. Zhang, A. Wang, M. Zhao, Y. Chen, L. Mei, and J. Wang, "Broadband few-layer MoS_2 saturable absorbers," Adv. Mater. **26**, 3538–3544 (2014).
61. K. Wang, Y. Feng, C. Chang, J. Zhan, C. Wang, Q. Zhao, J. N. Coleman, L. Zhang, W. Blau, and J. Wang, "Broadband ultrafast nonlinear absorption and nonlinear refraction of layered molybdenum dichalcogenide semiconductors," Nanoscale **6**, 10530–10535 (2014).
62. H. Liu, A. P. Luo, F. Z. Wang, R. Tang, M. Liu, Z. C. Luo, W. C. Xu, C. J. Zhao, and H. Zhang, "Femtosecond pulse erbium-doped fiber laser by a few-layer MoS_2 saturable absorber," Opt. Lett. **39**, 4591–4594 (2014).
63. J. Du, Q. Wang, G. B. Jiang, C. W. Xu, C. J. Zhao, Y. J. Xiang, Y. Chen, S. C. Wen, and H. Zhang, "Ytterbium-doped fiber laser passively mode locked by few-layer molybdenum disulfide (MoS_2) saturable absorber functioned with evanescent field interaction," Sci. Rep. **4**, 6346 (2014).
64. Z. Luo, Y. Huang, M. Zhong, Y. Li, J. Wu, B. Xu, H. Xu, Z. Cai, J. Peng, and J. Weng, "1-, 1.5-, and 2-μm fiber lasers *Q*-switched by a broadband few-layer MoS_2 saturable absorber," J. Lightwave Technol. **32**, 4679–4686 (2014).
65. M. Liu, X. W. Zheng, Y. L. Qi, H. Liu, A. P. Luo, Z. C. Luo, W. C. Xu, C. J. Zhao, and H. Zhang, "Microfiber-based few-layer MoS_2 saturable absorber for 2.5 GHz passively harmonic mode-locked fiber laser," Opt. Express **22**, 22841–22846 (2014).
66. Y. Huang, Z. Q. Luo, Y. Y. Li, M. Zhong, B. Xu, K. J. Che, H. Y. Xu, Z. P. Cai, J. Peng, and J. Weng, "Widely-tunable, passively *Q*-switched erbium-doped fiber laser with few-layer MoS_2 saturable absorber," Opt. Express **22**, 25258–25266 (2014).
67. H. Xia, H. Li, C. Lan, C. Li, X. Zhang, S. Zhang, and Y. Liu, "Ultrafast erbium-doped fiber laser mode-locked by a CVD-grown molybdenum disulfide (MoS_2) saturable absorber," Opt. Express **22**, 17341–17348 (2014).
68. R. Khazaeizhad, S. H. Kassani, H. Jeong, D.-I. Yeom, and K. Oh, "Mode-locking of Er-doped fiber laser using a multilayer MoS_2 thin film as a saturable absorber in both anomalous and normal dispersion regimes," Opt. Express **22**, 23732–23742 (2014).
69. R. I. Woodward, E. J. R. Kelleher, R. C. T. Howe, G. Hu, F. Torrisi, T. Hasan, S. V. Popov, and J. R. Taylor, "Tunable *Q*-switched fiber laser based on saturable edge-state absorption in few-layer molybdenum disulfide (MoS_2)," Opt. Express **22**, 31113–31122 (2014).
70. M. Zhang, R. C. T. Howe, R. I. Woodward, E. J. R. Kelleher, F. Torrisi, G. Hu, S. V. Popov, J. R. Taylor, and T. Hasan, "Solution processed MoS_2-PVA composite for sub-bandgap mode-locking of a wideband tunable ultrafast Er: fiber laser," Nano Res., doi: 10.1007/s12274-014-0637-2 (to be published).
71. Y. Wang, D. Mao, X. Gan, L. Han, C. Ma, T. Xi, Y. Zhang, W. Shang, S. Hua, and J. Zhao, "Harmonic mode locking of bound-state solitons fiber laser based on MoS_2 saturable absorber," Opt. Express **23**, 205–210 (2015).
72. R. Wang, H. C. Chien, J. Kumar, N. Kumar, H. Y. Chiu, and H. Zhao, "Third-harmonic generation in ultrathin films of MoS_2," ACS Appl. Mater. Interfaces **6**, 314–318 (2014).
73. S. T. Cundiff, B. C. Collings, N. N. Akhmediev, J. M. Soto-Crespo, K. Bergman, and W. H. Knox, "Observation of polarization-locked vector solitons in an optical fiber," Phys. Rev. Lett. **82**, 3988–3991 (1999).
74. D. Y. Tang, H. Zhang, L. M. Zhao, and X. Wu, "Observation of high-order polarization-locked vector solitons in a fiber laser," Phys. Rev. Lett. **101**, 153904 (2008).
75. H. Zhang, D. Y. Tang, L. M. Zhao, X. Wu, and H. Y. Tam, "Dissipative vector solitons in a dispersion managed cavity fiber laser with net positive cavity dispersion," Opt. Express **17**, 455–460 (2009).
76. L. M. Zhao, D. Y. Tang, X. Wu, H. Zhang, and H. Y. Tam, "Coexistence of polarization-locked and polarization-rotating vector solitons in a fiber laser with SESAM," Opt. Lett. **34**, 3059–3061 (2009).
77. Z. C. Luo, Q. Y. Ning, H. L. Mo, H. Cui, J. Liu, L. J. Wu, A. P. Luo, and W. C. Xu, "Vector dissipative soliton resonance in a fiber laser," Opt. Express **21**, 10199–10204 (2013).
78. D. Mao, X. M. Liu, and H. Lu, "Observation of pulse trapping in a near-zero dispersion regime," Opt. Lett. **37**, 2619–2621 (2012).
79. W. Chang, A. Ankiewicz, J. M. Soto-Crespo, and N. Akhmediev, "Dissipative soliton resonances," Phys. Rev. A **78**, 023830 (2008).
80. P. Grelu and N. Akhmediev, "Dissipative solitons for mode-locked lasers," Nat. Photonics **6**, 84–92 (2012).
81. X. Wu, D. Y. Tang, H. Zhang, and L. M. Zhao, "Dissipative soliton resonance in an all-normal-dispersion erbium-doped fiber laser," Opt. Express **17**, 5580–5584 (2009).
82. Z. C. Luo, W. J. Cao, Z. B. Lin, Z. R. Cai, A. P. Luo, and W. C. Xu, "Pulse dynamics of dissipative soliton resonance with large duration-tuning range in a fiber ring laser," Opt. Lett. **37**, 4777–4779 (2012).

83. X. H. Li, X. M. Liu, X. H. Hu, L. R. Wang, H. Lu, Y. S. Wang, and W. Zhao, "Long-cavity passively mode-locked fiber ring laser with high-energy rectangular-shape pulses in anomalous dispersion regime," Opt. Lett. **35**, 3249–3251 (2010).
84. X. Li, S. Zhang, H. Zhang, M. Han, F. Wen, and Z. Yang, "Highly efficient rectangular pulse emission in a mode-locked fiber laser," IEEE Photon. Technol. Lett. **26**, 2082–2085 (2014).
85. J.-H. Yang, C.-Y. Guo, S.-C. Ruan, D.-Q. Ouyang, H.-Q. Lin, Y.-M. Wu, and R.-H. Wen, "Observation of dissipative soliton resonance in a net-normal dispersion figure-of-eight fiber laser," IEEE Photon. J. **5**, 1500806 (2013).
86. C. Lecaplain, P. Grelu, J. M. Soto-Crespo, and N. Akhmediev, "Dissipative rogue waves generated by chaotic pulse bunching in a mode-locked laser," Phys. Rev. Lett. **87**, 2339108 (2013).
87. A. F. Runge, C. Aguergaray, N. G. Broderick, and M. Erkintalo, "Raman rogue waves in a partially mode-locked fiber laser," Opt. Lett. **39**, 319–322 (2014).
88. H. Zhang, D. Y. Tang, L. M. Zhao, and X. Wu, "Dark pulse emission of a fiber laser," Phys. Rev. A **80**, 045803 (2009).
89. Q. Y. Ning, S. K. Wang, A. P. Luo, Z. B. Lin, Z. C. Luo, and W. C. Xu, "Bright-dark pulse pair in a figure-eight dispersion-managed passively mode-locked fiber laser," IEEE Photon. J. **4**, 1647–1652 (2012).
90. S. Chouli and P. Grelu, "Rains of solitons in a fiber laser," Opt. Express **17**, 11776–11781 (2009).
91. F. Amrani, M. Salhi, P. Grelu, H. Leblond, and F. Sanchez, "Universal soliton pattern formations in passively mode-locked fiber lasers," Opt. Lett. **36**, 1545–1547 (2011).
92. Q. Y. Ning, H. Liu, X. W. Zheng, W. Yu, A. P. Luo, X. G. Huang, Z. C. Luo, W. C. Xu, S. H. Xu, and Z. M. Yang, "Vector nature of multi-soliton patterns in a passively mode-locked figure-eight fiber laser," Opt. Express **22**, 11900–11911 (2014).
93. Y. C. Meng, S. M. Zhang, X. L. Li, H. F. Li, J. Du, and Y. P. Hao, "Multiple-soliton dynamic patterns in a graphene mode-locked fiber laser," Opt. Express **20**, 6685–6692 (2012).
94. P. F. Zhu, Z. B. Lin, Q. Y. Ning, Z. R. Cai, X. B. Xing, J. Liu, W. C. Chen, Z. C. Luo, A. P. Luo, and W. C. Xu, "Passive harmonic mode-locking in a fiber laser by using a microfiber-based graphene saturable absorber," Laser Phys. Lett. **10**, 105107 (2013).
95. D. Y. Tang, L. M. Zhao, B. Zhao, and A. Q. Liu, "Mechanism of multisoliton formation and soliton energy quantization in passively mode-locked fiber lasers," Phys. Rev. A **72**, 043816 (2005).
96. A. Komarov, H. Leblond, and F. Sanchez, "Multistability and hysteresis phenomena in passively mode-locked fiber lasers," Phys. Rev. A **71**, 053809 (2005).
97. A. Zavyalov, R. Iliew, O. Egorov, and F. Lederer, "Dissipative soliton molecules with independently evolving or flipping phases in mode- locked fiber lasers," Phys. Rev. A **80**, 043829 (2009).
98. M. Grapinet and P. Grelu, "Vibrating soliton pairs in a mode-locked laser cavity," Opt. Lett. **31**, 2115–2117 (2006).
99. S. Chouli and P. Grelu, "Soliton rains in a fiber laser: an experimental study," Phys. Rev. A **81**, 063829 (2010).
100. F. Amrani, A. Haboucha, M. Salhi, H. Leblond, A. Komarov, and F. Sanchez, "Dissipative solitons compounds in a fiber laser. Analogy with the states of the matter," Appl. Phys. B **99**, 107–114 (2010).
101. Z. C. Luo, W. C. Xu, C. X. Song, A. P. Luo, and W. C. Chen, "Modulation instability induced by periodic power variation in soliton fiber ring lasers," Eur. Phys. J. D **54**, 693–697 (2009).
102. D. Y. Tang, L. M. Zhao, X. Wu, and H. Zhang, "Soliton modulation instability in fiber lasers," Phys. Rev. A **80**, 023806 (2009).
103. Y. Meng, A. Niang, K. Guesmi, M. Salhi, and F. Sanchez, "1.61 μm high-order passive harmonic mode locking in a fiber laser based on graphene saturable absorber," Opt. Express **22**, 29921–29926 (2014).
104. A. Komarov, K. Komarov, A. Niang, and F. Sanchez, "Nature of soliton interaction in fiber lasers with continuous external optical injection," Phys. Rev. A **89**, 013833 (2014).
105. H. Zhang, S. Virally, Q. L. Bao, L. K. Ping, S. Massar, N. Godbout, and P. Kockaert, "*Z*-scan measurement of the nonlinear refractive index of graphene," Opt. Lett. **37**, 1856–1858 (2012).
106. S. B. Lu, C. J. Zhao, Y. H. Zou, S. Q. Chen, Y. Chen, Y. Li, H. Zhang, S. C. Wen, and D. Y. Tang, "Third order nonlinear optical property of Bi_2Se_3," Opt. Express **21**, 2072–2082 (2013).